Original paper

Fluorpyromorphite, $Pb_5(PO_4)_3F$, a new apatite-group mineral from Sukhovyaz Mountain, Southern Urals, and Tolbachik volcano, Kamchatka

Anatoly V. KASATKIN[1]*, Igor V. PEKOV[2], Radek ŠKODA[3], Nikita V. CHUKANOV[4], Fabrizio NESTOLA[5], Atali A. AGAKHANOV[1], Aleksey M. KUZNETSOV[6], Natalia N. KOSHLYAKOVA[3], Jakub PLÁŠIL[7], Sergey N. BRITVIN[8]

[1] *Fersman Mineralogical Museum of Russian Academy of Sciences, Leninsky Prospekt 18–2, 119071 Moscow, Russia; anatoly.kasatkin@gmail.com*
[2] *Faculty of Geology, Moscow State University, Vorobievy Gory, 119991 Moscow, Russia*
[3] *Department of Geological Sciences, Faculty of Science, Masaryk University, Kotlářská 2, 611 37, Brno, Czech Republic*
[4] *Federal Research Center of Problems of Chemical Physics and Medicinal Chemistry, Russian Academy of Sciences, Chernogolovka, 142432, Moscow Region, Russia*
[5] *Dipartimento di Geoscienze, Università di Padova, Via Gradenigo 6, I-35131, Padova, Italy*
[6] *Oktyabrskaya str., 5-337, 454071 Chelyabinsk, Russia*
[7] *Institute of Physics of the CAS, v.v.i, Na Slovance 1999/2, 182 21, Prague 8, Czech Republic*
[8] *Dept. of Crystallography, St Petersburg State University, University Embankment 7/9, 199034 St Petersburg, Russia*
**Corresponding author*

Fluorpyromorphite, ideally $Pb_5(PO_4)_3F$, a new apatite-group member, an F-dominant analog of pyromorphite and hydroxylpyromorphite. It is a supergene mineral found at two localities: Sukhovyaz Mountain, Ufaley District, Southern Urals (holotype) and Mountain 1004, Tolbachik volcano, Kamchatka (co-type), both in Russia. At Sukhovyaz, fluorpyromorphite forms anhedral grains up to 0.2 mm across (usually much smaller), filling cavities in quartz and sometimes partially replacing fluorapatite. Associated supergene minerals include pyromorphite, hydroxylpyromorphite, fluorphosphohedyphane, mimetite, and nickeltsumcorite. At Tolbachik, fluorpyromorphite occurs in the oxidation zone of paleo-fumarolic deposits in close association with pyromorphite, fluorphosphohedyphane, wulfenite, cerussite, munakataite, vanadinite, chrysocolla, and opal. It forms crude long-prismatic to acicular crystals up to 0.1 mm long and up to 5 μm thick combined in bunches and spherulites up to 0.2 mm. Fluorpyromorphite is colorless (Sukhovyaz) or yellow (Tolbachik), translucent to transparent and has a vitreous luster. It is brittle, with an uneven fracture and poor cleavage on (001). The calculated density values are 7.382 (holotype) and 6.831 (cotype) g/cm^3. Fluorpyromorphite is optically uniaxial (–). In reflected light, it is light-grey, weakly anisotropic. The reflectance values (R_{min}/R_{max}, %) are: 15.8/16.6 (470 nm), 16.2/17.2 (546 nm), 15.9/16.9 (589 nm), 15.4/16.2 (650 nm). The chemical composition is (electron microprobe, wt. %; holotype/co-type): CaO 0.10/3.16, SrO 0.17/0.00, PbO 83.51/77.39, P_2O_5 16.13/16.35, CrO_3 0.00/0.49, SeO_3 0.00/0.98, F 1.00/1.35, Cl 0.29/0.40, H_2O_{calc} 0.13/0.00, –O=(F,Cl) –0.49/–0.66, total 100.84/99.46. The empirical formulae based on 13 anions (O+F+Cl+OH) *pfu* are $Pb_{4.95}Ca_{0.02}Sr_{0.02}P_{3.00}O_{12}F_{0.70}(OH)_{0.19}Cl_{0.11}$ (holotype) and $Pb_{4.26}Ca_{0.69}P_{2.83}Se^{6+}_{0.09}Cr^{6+}_{0.06}O_{11.99}F_{0.87}Cl_{0.14}$ (co-type). Fluorpyromorphite is hexagonal, space group $P6_3/m$, unit-cell parameters (from powder X-ray diffraction data; holotype / co-type) are: a = 9.779(5) / 9.732(1), c = 7.241(9) / 7.242(1) Å, V = 599.6(7) / 594.0(2) Å^3, and Z = 2. The crystal structure was refined using the Rietveld method to R_p = 0.1764 (holotype). Fluorpyromorphite is isostructural with other members of the apatite group, a subdivision of the apatite supergroup.

Keywords: fluorpyromorphite, new mineral, apatite group, Sukhovyaz Mountain, Southern Urals, Tolbachik volcano
Received: 24 October 2022; accepted: 8 December 2022; handling editor: M. Števko

1. Introduction

The apatite supergroup includes numerous minerals with the general formula $^{IX}\mathbf{M1}_2{}^{VII}\mathbf{M2}_3(^{IV}\mathbf{T}O_4)_3\mathbf{X}$. Their crystal structures are based upon a heteropolyhedral framework of metal cations (**M**) and tetrahedrally coordinated (**T**) atoms and contain columns of the additional **X** anions. The general formula of minerals belonging to the apatite group, one of the five within the namesake supergroup, can be written shortly as $\mathbf{M}_5(\mathbf{T}O_4)_3\mathbf{X}$, because the same prevailing cation occurs at both M1 and M2 sites (Pasero et al. 2010). The species-defining components of valid apatite-group minerals are as follows: **M** = Ca, Mn^{2+}, Sr, Ba, Pb^{2+}; **T** = P, V^{5+}, As^{5+}; **X** = F^-, $(OH)^-$ and Cl^- (Pasero et al. 2010; Tait et al. 2015). To date, this group contains fourteen species: eight phosphates (fluorapatite, hydroxylapatite, chlorapatite, pyromorphite, hydroxylpyromorphite, alforsite, stronadelphite and pieczkaite), four

arsenates (johnbaumite, mimetite, svabite and turneaurite) and two vanadates (vanadinite and pliniusite).

Fluorpyromorphite (Russian Cyrillic фторпироморфит) described herein is, therefore, the fifteenth mineral and ninth phosphate of the group with the following combination of species-defining constituents: **M** = Pb, **T** = P and **X** = F. It is named as the analog of pyromorphite and hydroxylpyromorphite with dominant fluorine at the **X** anionic site. The prefix "fluor" is used in line with the common nomenclature scheme for the apatite supergroup (Pasero et al. 2010).

The new mineral, its name and symbol (Fpym) have been approved by the Commission on New Minerals, Nomenclature and Classification (CNMNC) of the International Mineralogical Association (IMA 2021–120). The holotype specimen is deposited in the collections of the Fersman Mineralogical Museum of the Russian Academy of Sciences, Moscow, Russia, with catalog number 97915.

2. Occurrence and mineral associations

The new mineral was found at two localities situated in different regions of Russia. The holotype originates from the Sukhovyaz Mt., Ufaley District, approximately 2.5 km SW of the city of Verkhniy Ufaley, Chelyabinsk Oblast, Southern Urals. The cotype locality is the Tolbachik volcano at Kamchatka.

2.1. Sukhovyaz Mountain

The material which became the holotype of fluorpyromorphite was collected in May 2021 by one of the authors (A.M.K.) at the Area #2 of the small Sukhovyaz (Sukhovyazskoe) lead deposit located at the southern slope of the Sukhovyaz Mt. (Fig. 1). GPS-coordinates of the sampling site are 56°1'55" N and 60°10'57" E.

Fig. 1 Sukhovyaz Mt., Sukhovyaz deposit, Area #2. Photo: S.G. Epanchintsev, summer 2021.

Sukhovyaz Mt. is built mainly by granites, gneisses and crystalline schists, which host hydrothermal quartz veins with sulfides. In Area # 2 (*c.* 0.6×0.6 km^2) occur mainly quartz–mica–chlorite schists and micaceous quartzites. In places, they alternate with talc–carbonate rocks, serpentinites and subordinate listvenites surrounding quartz veins (Fig. 2). The largest quartz vein, about 10 m thick, stretches from west to east. Embedding rocks are composed of greenish talc schists, replaced by mica and graphite schists in the north and south. Quartz in the main vein is crosscut by a network of cracks that strike 315° NW and dip 51° NE.

The common ore minerals of the vein are galena, pyrite and chalcopyrite. In addition, supergene mineralization is distributed inside the quartz veins. The main minerals of the oxidation zone are anglesite, cerussite, crocoite, goethite, malachite, plumbojarosite, vauquelinite and especially pyromorphite. Pyromorphite is undoubtedly the most famous mineral of the locality: it was first found here in 1897 and since then has been a subject of detailed crystallographic, optical and chemical studies (Pertel 1950; Vertushkov 1958; Vlasov 2010; Popov and Krainev 2013). Specimens with dark-green prismatic crystals of Sukhovyaz pyromorphite reaching 1 cm in length and their spectacular clusters and crusts on quartz matrix adorn many museums and private collections.

The new mineral was discovered during routine SEM/EDS examination of the samples of massive milky-white quartz. Macroscopically, the latter is overgrown by green prismatic pyromorphite crystals up to 5 mm and contains Ag-rich gold (up to 21 wt. % Ag, $Au_{0.66}Ag_{0.34}$) inclusions up to 1 mm. Fluorpyromorphite was discovered in two polished sections in minor amounts. Its grains and their aggregates fill small caverns in quartz. Some grains of fluorpyromorphite contain zones poor in F and Cl and, thus, are considered to correspond to hydroxylpyromorphite. Other supergene minerals found in close association with fluorpyromorphite are acanthite, fluorphosphohedyphane, mimetite, and nickeltsumcorite, whereas the primary assemblage includes fluorapatite, gersdorffite, monazite-(Ce), muscovite, rutile, and zircon.

2.2. Tolbachik volcano

The co-type material was collected by one of the authors (I.V.P.) at the Western paleo-fumarole field located at the western slope of Mountain 1004, a scoria cone situated 20 km SSW of the Ploskiy Tolbachik active volcano, Kamchatka (55°40'19" N and 160°14'07" E). Mountain 1004 is one of the numerous monogenetic volcanoes belonging to the Tolbachik volcanic complex. This scoria cone was formed due to an ancient basalt eruption of

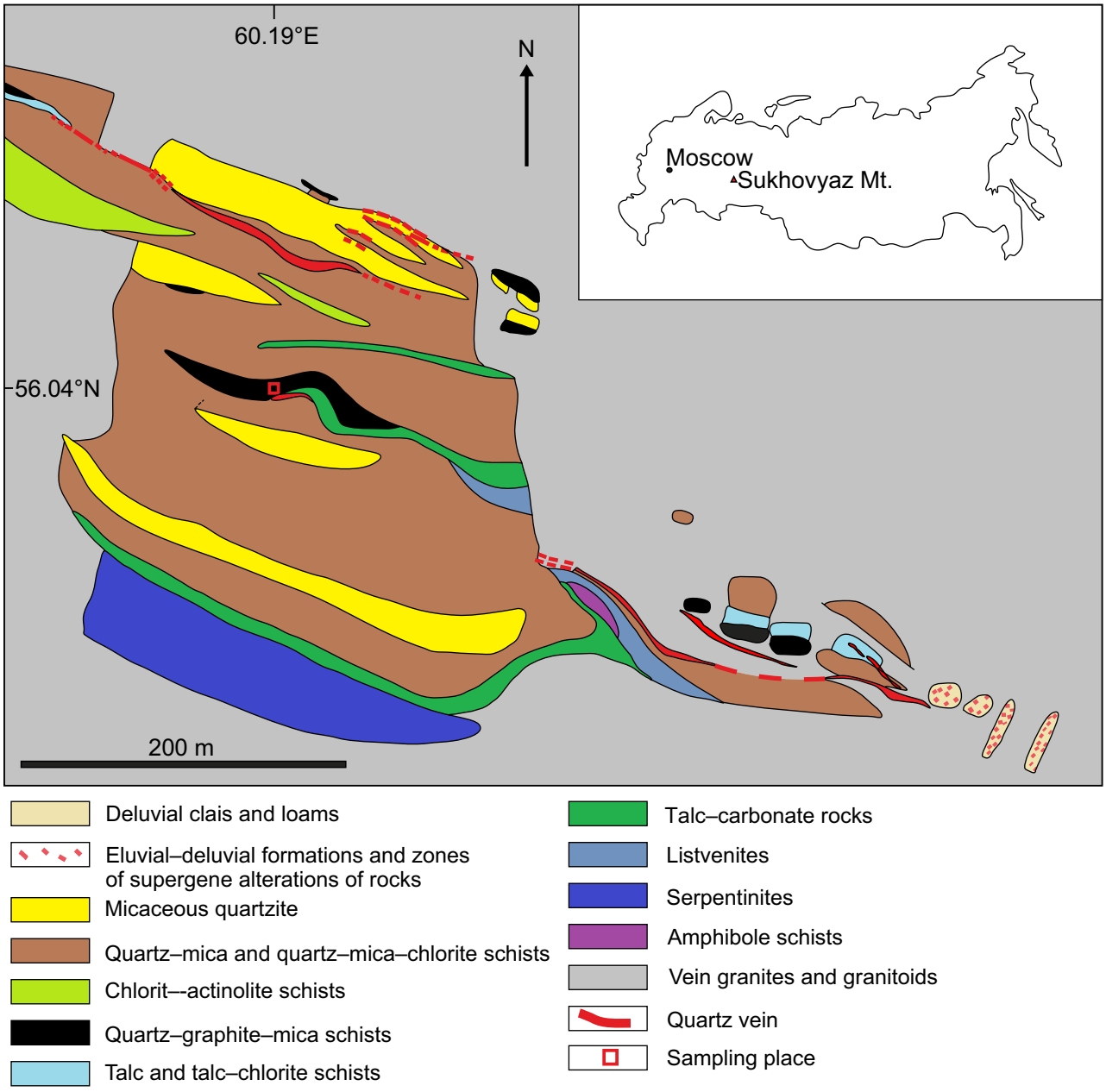

Fig. 2 Geographic location and geological sketch map of Area #2 of the Sukhovyaz deposit, Sukhovyaz Mt. (based on the 1952 Geological Report of the Ufalei Prospecting Crew).

the Plinian type approximately two thousand years ago (Fedotov and Markhinin 1983 eds). Now all fumaroles at Mountain 1004 are extinct, and a weathered zone formed on the paleo-fumarolic fields during this period. These fumaroles belonged to the oxidizing type, like the well-studied active fumaroles associated with the Great Tolbachik Fissure Eruption (GTFE) of 1975–1976 (Pekov et al. 2020), and likewise produced rich "ore" sublimate mineralization. Some exhalation minerals, relatively stable to weathering, are preserved in deposits of paleo-fumaroles of Mountain 1004. To date can be found, e.g., hematite, tenorite, magnesioferrite, feldspars, diopside, and fluorophlogopite (Shchipalkina et al. 2020). Based on both the analogy with the mineralization occurring now in active fumaroles of GTFE and the chemistry of supergene minerals found in the oxidation zone of paleo-fumaroles of Mountain 1004, we conclude that the "ore" sublimate assemblages at the Western and Southern fumarole fields at Mountain 1004 initially included oxysalts and halides unstable in air with not only Cu but also with Pb, Se, As, V, and Mo. The most abundant secondary minerals in the oxidation zone of the Western paleo-fumarole field are chrysocolla, atacamite (both giving the characteristic bright green or bluish-green coloration to the surface of

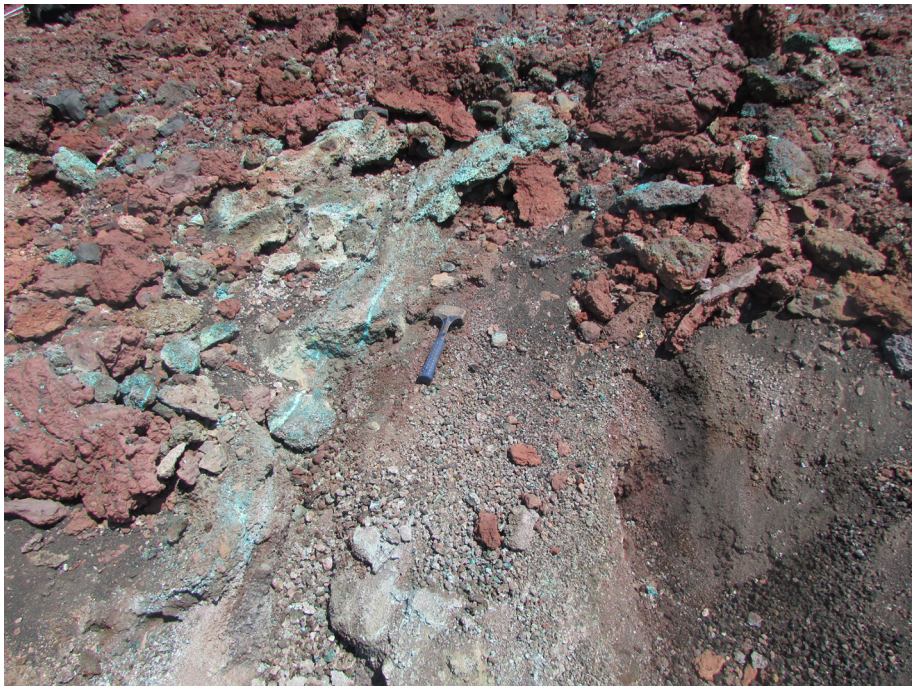

Fig. 3 Surface of the Western paleo-fumarole field at Mountain 1004 (Tolbachik volcano) in which fluorpyromorphite was found. Red–brown boulders are basalt volcanic bombs altered by fumarolic gas and partially hematitized; green areas are enriched with chrysocolla and atacamite. Photo: M. O. Bulakh, summer 2022.

the weathered "ore" areas of paleo-fumarolic deposits: Fig. 3), opal, gypsum, fluorite, and X-ray amorphous allophane-like Al silicate. Supergene lead minerals are not abundant but diverse: there are cerussite, anglesite, linarite, munakataite, wulfenite, phoenicochroite, mottramite, murdochite, and apatite-group members represented by vanadinite, pyromorphite, fluorphosphohedyphane and fluorpyromorphite. We did not find relics of primary lead minerals at this locality but can suggest that the sublimate lead sulfates or chlorides were a source of Pb, by analogy with the active GTFE fumaroles in which anglesite, palmierite and cotunnite are common.

3. General appearance, physical properties and optical data

At Sukhovyaz, fluorpyromorphite occurs as anhedral grains filling small cavities in quartz. The grain depicted in Fig. 4 is the largest found. It measures *c.* 0.2×0.15 mm^2 in section and was used to obtain most of the analytical data (chemical, optical, X-ray diffraction, Raman spectroscopy) for the holotype of the new mineral. Other observed grains do not exceed 0.05 mm. Some of fluorpyromorphite grains replace fluorapatite and contain its relics. The holotype fluorpyromorphite

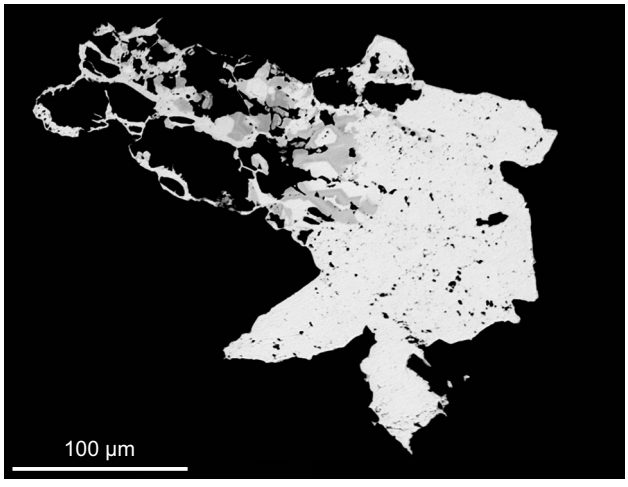

Fig. 4 Fluorpyromorphite (white) grains partially replaced by fluorapatite (grey) among quartz (black) from Sukhovyaz Mt. This grain is the holotype used for electron-microprobe analyses, Raman spectroscopy, reflectance measurements and X-ray diffraction studies. Back-Scattered Electrons (BSE) image.

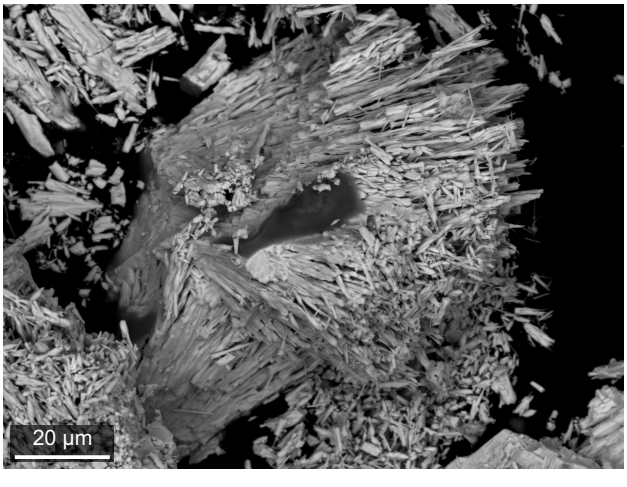

Fig. 5 Bunches of crude long-prismatic crystals of fluorpyromorphite from the Tolbachik volcano (co-type). Back-Scattered Electrons (BSE) image.

is colorless, translucent, and has a vitreous luster and a white streak.

At Tolbachik, fluorpyromorphite is found in cavities of aggregates mainly composed by chrysocolla, opal and allophane-like Al silicate. The new mineral forms crude long-prismatic to acicular crystals up to 0.1 mm long and up to 5 μm thick combined in bunches and dense or open-work radial spherulites (Fig. 5) up to 0.2 mm across. Some spherulites of fluorpyromorphite have marginal parts represented by pyromorphite (with Cl > F in atom proportions). Other minerals closely associated with fluorpyromorphite and pyromorphite are fluorphosphohedyphane, wulfenite, cerussite, munakataite, and vanadinite. The Tolbachik fluorpyromorphite is transparent to translucent, pale yellow, bright yellow, or, in cores of some spherulites, green-yellow with an olive hue. In addition, it has a strong vitreous luster.

Fluorpyromorphite is brittle, with an uneven fracture (observed under the scanning electron microscope). The cleavage is poor on (001) and parting is not observed. The mineral is non-fluorescent under ultraviolet light. The Mohs' hardness is suggested as 3½–4, by analogy with pyromorphite. The density could not be measured because of the absence of available heavy liquids and the paucity of material. The calculated density based on the empirical formulae and PXRD data is 7.382 and 6.831 g/cm^3 for the holotype from Sukhovyaz and co-type from Tolbachik, respectively. This difference is caused by the difference in cationic composition: the co-type contains more admixed Ca, which substitutes much heavier Pb (see Section 5).

Optically, fluorpyromorphite is uniaxial negative. Its refractive indices (RI) could not be measured because of the very small amount of available material and the absence of immersion liquids that can measure RI values greater than 2. The Gladstone–Dale relationship predicts an average index of refraction of *c*. 2.04. Optical properties were studied for the holotype using the methods common for metallic minerals. In reflected light, the new mineral is light-grey. Bireflectance and pleochroism were not observed. Under crossed polars, it is very weakly anisotropic with no visible internal reflections. Reflectance spectra were measured in air with a Universal Microspectrophotometer UMSP 50 (Opton-Zeiss, Germany) using a SiC standard. The results from the 400–700 nm range are given in Tab. 1 and plotted in Fig. 6.

Tab. 1 Reflectance values of fluorpyromorphite (holotype, measured in air)

R_{max}	R_{min}	λ (nm)	R_{max}	R_{min}	λ (nm)
15.8	15.5	400	17.2	16.1	560
15.8	15.6	420	17.0	16.0	580
16.1	15.7	440	16.9	15.9	589 (COM)
16.4	15.7	460	16.8	15.9	600
16.6	15.8	470 (COM)	16.5	15.7	620
16.8	15.8	480	16.2	15.5	640
17.2	16.0	500	16.2	15.4	650 (COM)
17.3	16.1	520	16.1	15.3	660
17.4	16.2	540	16.0	15.2	680
17.3	16.2	546 (COM)	15.7	15.1	700

COM = Commission on Ore Mineralogy of the International Mineralogical Association

4. Raman spectroscopy

The Raman spectrum of the holotype fluorpyromorphite (Fig. 7) was obtained by means of a Horiba Labram HR Evolution spectrometer. This dispersive, edge-filter-based system is equipped with an Olympus BX 41 optical microscope, a diffraction grating with 600 grooves per millimeter, and a Peltier-cooled, Si-based charge-coupled device (CCD) detector. After careful tests with different

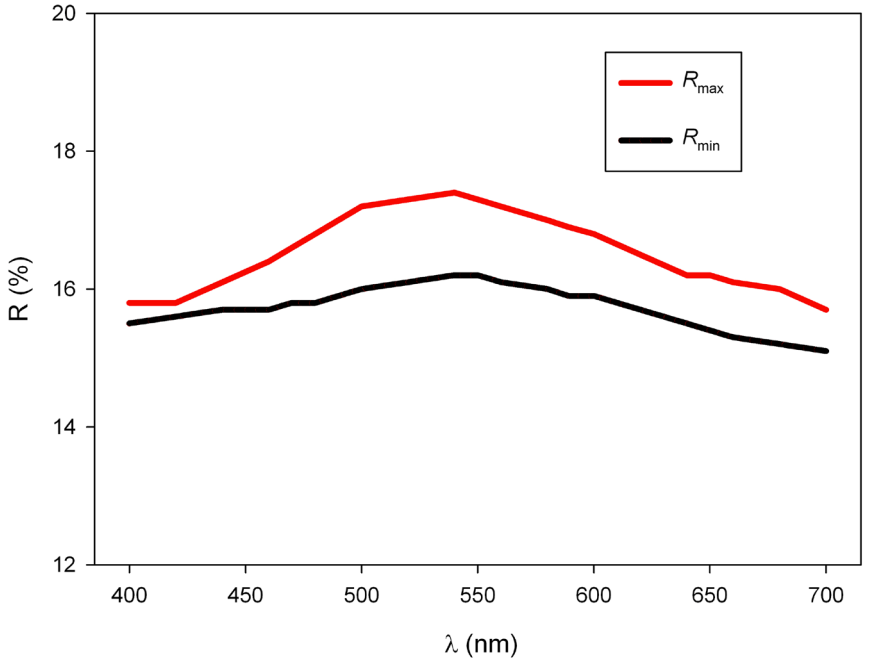

Fig. 6 Reflectivity curves for fluorpyromorphite (holotype) in air.

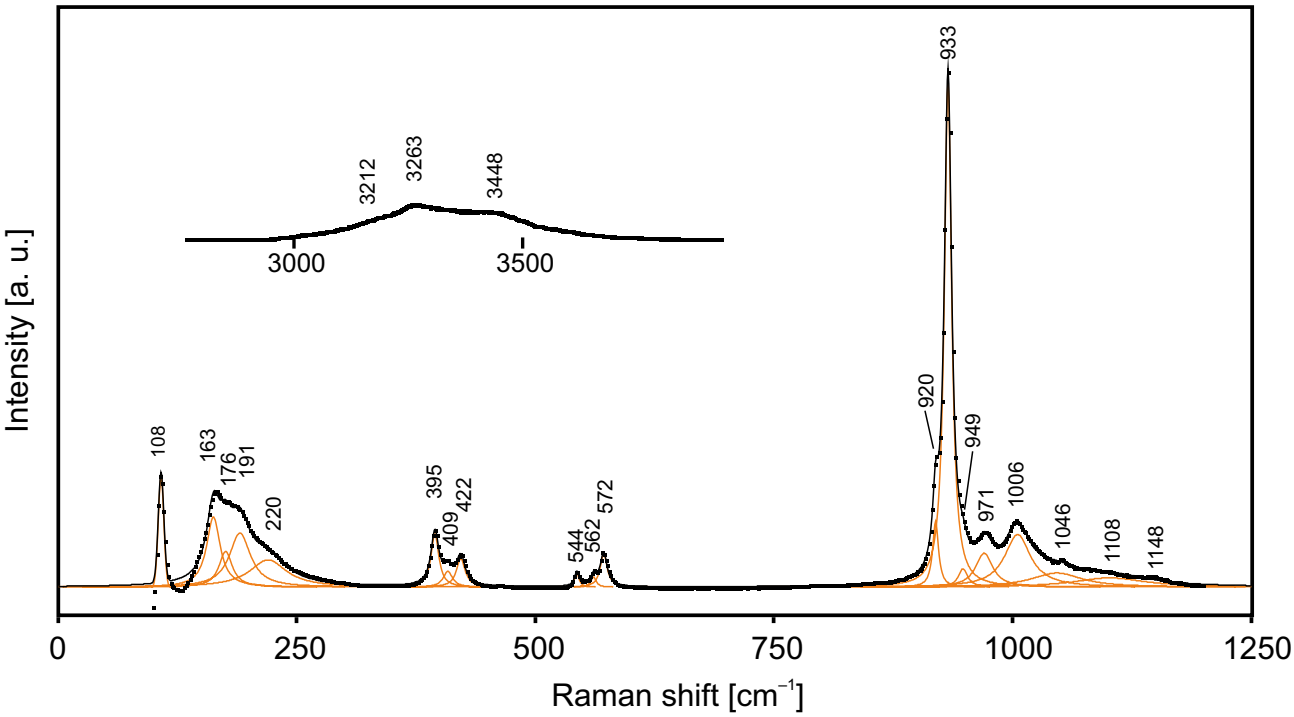

Fig. 7 Raman spectrum of fluorpyromorphite (holotype) excited by 532 nm laser: in the 100–1250 and 3000–3600 cm^{-1} regions. Dots represent the collected spectral data. The black curve matching to dots results from spectral fit as a sum of individual Voigt peaks (orange).

lasers (473, 532 and 633 nm), the 532 nm diode-based laser with the beam power of 20 mW at the sample surface was selected for spectra acquisition to minimize analytical artifacts. Raman signal was collected in the range of 100–4000 cm^{-1} with a 100× objective and the system is operated in the confocal mode, the beam diameter was ~0.7 μm and the depth resolution ~2 μm. No visual damage to the analyzed surface was observed at these conditions after the excitation. Wavenumber calibration was done using the Rayleigh line and low-pressure Ne-lamp emissions. The wavenumber accuracy was ~0.5 cm^{-1}, and the spectral resolution was ~2 cm^{-1}. Band fitting was done after appropriate background correction, assuming combined Lorentzian–Gaussian band shapes using the Voigt function (*PeakFit*; Jandel Scientific Software).

The assignment of the Raman bands is as follows. The range of 3200–3500 cm^{-1} corresponds to O–H stretching vibrations. The bands at 971 and 1006 cm^{-1} are due to asymmetric stretching vibrations of PO_4^{3-} anions [the $F_2(\nu_3)$ mode]. The presence of these bands in the Raman spectrum indicates that the PO_4 tetrahedron is slightly distorted. The band at 933 cm^{-1} is attributed to symmetric stretching vibrations of two non-equivalent PO_4^{3-} [the $A_1(\nu_1)$ mode]. The shoulders at 920 and 949 cm^{-1} may correspond to a subordinate local situation involving Ca, Sr, OH and/or Cl. The range of 540–580 cm^{-1} is assigned to PO_4^{3-} bending [the $F_2(\nu_4)$ mode] vibrations. The range of 390–430 cm^{-1} is due to PO_4^{3-} bending [the $E(\nu_2)$ mode] vibrations. Raman bands observed below 250 cm^{-1} correspond to lattice modes involving vibrations PO_4^{3-} groups as a whole (acoustic modes) and Pb–O bonds. Very weak Raman bands at 1108 and 1148 cm^{-1} and the weak band at 1046 cm^{-1} are assigned to combination modes and overtone of non-equivalent $F_2(\nu_4)$ components due to the distortion of the PO_4 tetrahedron. The band assignment was made in accordance with Levitt and Condrate (1970), Adams and Gardner (1974), Bartholomäi and Klee (1978), Botto et al. (1997), and Bajda et al. (2011). No Raman bands are observed in the range of 1200–3000 cm^{-1}.

5. Chemical composition

The chemical composition of fluorpyromorphite and associated apatite-supergroup minerals (Tab. 2) was determined by electron microprobe in the wavelength-dispersive (WDS) mode. The specimens from Sukhovyaz were studied using a Cameca SX-100 electron microprobe (Masaryk University, Brno, Czech Republic = MU) operated at 15 kV and 4 nA with a beam size of 5 μm. Peak counting times were 20 s for all elements, with one-half of the peak time for each background. The specimens from Tolbachik were analyzed using a Jeol JSM-6480LV scanning electron microscope equipped with an INCA-Wave 500 spectrometer (Laboratory of Analytical Techniques of High Spatial Resolution, Dept. of Petrology, Moscow State University, Russia = MSU),

Tab. 2 Chemical composition of fluorpyromorphite and associated apatite-supergroup minerals from Sukhovyaz Mt., South Urals (1–7) and Tolbachik volcano, Kamchatka (8–11)

Constituent	Sukhovyaz							Tolbachik			
	1	2	3	4	5	6	7	8	9	10	11
wt. %											
CaO	0.10 (0.00–0.32)	0.15	0.05	0.34	7.87	52.63	0.25	3.16	2.06	–	7.23
SrO	0.17 (0.11–0.20)	–	–	–	–	1.44	–	–	–	–	–
PbO	83.51 (82.79–84.40)	82.50	83.20	82.34	70.15	1.75	73.78	77.39	79.61	78.55	72.38
P_2O_5	16.13 (16.00–16.23)	15.90	16.05	16.02	19.32	41.13	–	16.35	16.52	0.61	19.13
V_2O_5	–	–	–	–	–	–	–	–	–	17.71	–
As_2O_5	–	–	–	–	–	–	23.55	–	–	–	–
CrO_3	–	–	–	–	–	–	–	0.49	–	0.47	–
SeO_3	–	–	–	–	–	–	–	0.98	0.90	–	–
F	1.00 (0.92–1.06)	1.36	0.37	0.14	1.70	3.68	–	1.35	0.05	–	1.63
Cl	0.29 (0.11–0.56)	–	0.52	2.01	–	–	2.40	0.40	2.24	2.59	0.07
H_2O_{calc}*	0.13	0.03	0.37	0.10	0.04	–	–		0.13		0.03
–O=(F,Cl)	–0.49	–0.57	–0.27	–0.51	–0.72	–1.55	–0.54	–0.66	–0.53	–0.59	–0.70
Total	100.84	99.37	100.29	100.44	98.36	99.08	99.44	99.46	100.98	99.34	99.77
formulae calculated on the basis of 13 anions (O + F + Cl + OH) *pfu*											
Ca	0.02	0.04	0.01	0.08	1.55	4.87	0.07	0.69	0.46	–	1.43
Sr	0.02	–	–	–	–	0.07	–	–	–	–	–
Pb	4.95	4.95	4.96	4.91	3.46	0.04	4.88	4.26	4.47	5.02	3.60
P	3.00	3.00	3.01	3.00	3.00	3.01	–	2.83	2.92	0.12	2.99
V^{5+}	–	–	–	–	–	–	–	–	–	2.78	–
As^{5+}	–	–	–	–	–	–	3.02	–	–	–	–
Cr^{6+}	–	–	–	–	–	–	–	0.06	–	0.07	–
Se^{6+}	–	–	–	–	–	–	–	0.09	0.09	–	–
O	12.00	12.00	12.00	12.00	12.00	12.00	12.00	11.99	12.00	11.96	12.00
F	0.70	0.96	0.26	0.10	0.99	1.01	–	0.87	0.03	–	0.95
Cl	0.11	–	0.20	0.75	–	–	1.00	0.14	0.79	1.04	0.02
OH*	0.19	0.04	0.54	0.15	0.01	–	–		0.18		0.03
ΣM	4.99	4.99	4.97	4.99	5.01	4.98	4.95	4.95	4.93	5.02	5.03
ΣT	3.00	3.00	3.01	3.00	3.00	3.01	3.02	2.98	3.01	2.97	2.99

1, 2, 8 – fluorpyromorphite (1 – holotype, mean of 8 spot analyses, ranges are in parentheses; 2 – F-richest spot; 8 – cotype); 3 – hydroxylpyromorphite (mean of 4 spot analyses); 4, 9 – pyromorphite (4 – mean of 75 spot analyses); 5, 11 – fluorphosphohedyphane; 6 – fluorapatite; 7 – mimetite; 10 – vanadinite.

ΣM = Ca + Sr + Pb, ΣT = P + V + As + Cr + Se

*H_2O content is calculated for analyses with (F + Cl) < 1.00 *apfu* based on the assumption that all H_2O corresponds to hydroxyl groups and (F + Cl + OH) = 1.00 *pfu*. –: below the detection limit

with an acceleration voltage of 20 kV, a beam current of 20 nA, and a 3 μm beam diameter. The following standards were used (MU/MSU): Ca: wollastonite/diopside; Sr: $SrSO_4$/–; Pb, Cl: vanadinite/vanadinite; P: fluorapatite/$LaPO_4$; Cr: –/Cr; Se: –/Se; F: topaz/MgF_2. In the case of MU, the F content was determined using PC1 monochromator ($2d$ = 60 Å) and special care was paid to the peak-maxima position and background selection prior to the analysis. Anisotropic behavior of F K_α X-ray emission in apatites varies with crystal orientation and intensity of the electron exposure, which complicates the precise analysis of F by electron-beam techniques (e.g., Stormer et al. 1993, Goldoff et al. 2012). To avoid overestimation of the F content, mild analytical conditions were used, and the extrapolation of the FK_α X-ray count rate to time zero was applied. Raw X-ray intensities were corrected for matrix effects with a $\phi(\rho z)$ algorithm of the X–PHI routine (Merlet 1994). No other elements with atomic numbers higher than 4 (beryllium) were detected. Water content was not determined directly due to the scarcity of pure material.

The empirical formulae were calculated based on 13 anions (O + F + Cl + OH) *pfu*, with the assumption that (F + Cl + OH) = 1.00 *pfu* in samples with (F + Cl) < 1.00 *apfu*. The empirical formulae of fluorpyromorphite are as follows. Holotype from Sukhovyaz: $Pb_{4.95}Ca_{0.02}Sr_{0.02}$

$P_{3.00}O_{12}F_{0.70}(OH)_{0.19}Cl_{0.11}$; co-type from Tolbachik: $Pb_{4.26}Ca_{0.69}P_{2.83}Se^{6+}_{0.09}Cr^{6+}_{0.06}O_{11.99}F_{0.87}Cl_{0.14}$. Thus, the Sukhovyaz samples contain the mineral close to the end member concerning **M** and **T** components, while at Tolbachik fluorpyromorphite is represented by a Ca-, Se- and Cr-bearing variety. Admixed Se and Cr are suggested as Se^{6+} and Cr^{6+} by analogy with synthetic apatite-type compounds in which these elements occur in the form of tetrahedral selenate SeO_4^{2-} and chromate CrO_4^{2-} groups (White et al. 2005).

The idealized, end-member formula of fluorpyromorphite is $Pb_5(PO_4)_3F$ which requires PbO 83.29, P_2O_5 15.89, F 1.42, –O = F –0.60, total 100 wt. %.

6. X-ray crystallography

Single-crystal X-ray diffraction (XRD) studies could not be carried out because no suitable single crystal was found in the material from both localities. For this reason, XRD data for both holotype and co-type specimens were collected in powder diffraction mode (Tab. 3).

The holotype specimen from Sukhovyaz was studied using a Supernova single-crystal X-ray Rigaku-Oxford Diffraction diffractometer equipped with a Pilatus 200 K Dectris detector and an X-ray micro-source (MoK_α radiation) with a spot size of ~0.12 mm. The detector-to-sample distance was 68 mm. A standard phi-scan mode as implemented in the powder power tool of CrysAlisPro was used for the powder data collection. We collected 1196 frames, 0.3° and 40 seconds of exposure per frame for a total of about 13 hours of data collection, reaching a minimum *d*-spacing equal to 1.10 Å. The least-squares refinement of the unit cell, based on individually fitted d_{hkl} spacings obtained by profile fitting in the High-Score Plus program (PANalytical, Almelo, Netherlands), using the pseudo-Voigt shape function, was performed with the Unit-cell software (Holland and Redfern 1997). Unit-cell parameters refined based on the single-profile fitting from the powder data are as follows: fluorpyromorphite is hexagonal, space group $P6_3/m$ (#176), a = 9.779(5), c = 7.241(9) Å, V = 599.6(7) Å^3, and Z = 2.

Powder XRD data of co-type specimen from Tolbachik were collected with a Rigaku R-AXIS Rapid II diffractometer equipped with a cylindrical image plate detector (r = 127.4 mm) using Debye–Scherrer geometry, CoK_α radiation (rotating anode with VariMAX microfocus optics), 40 kV, 15 mA and an exposure time of 15 min. The angular resolution of the detector is 0.045 2Θ (pixel size 0.1 mm). The data were integrated using the Osc2Tab software package (Britvin et al. 2017). The hexagonal unit-cell parameters are: a = 9.732(1), c = 7.242(1) Å, and V = 594.0(2) Å^3. Slightly decreased unit-cell dimensions of this sample compared to holotype are caused by both distinct Ca admixture and higher F:Cl ratio in co-type (Tab. 2, analysis #8). Powder XRD data for pyromorphite closely associated with fluorpyromorphite from Tolbachik were obtained under the same conditions. Its hexagonal unit cell has the following parameters: a = 9.984(4), c = 7.353(3) Å, and V = 634.8(7) Å^3.

Tab. 3 Powder X-ray diffraction data (d in Å) of fluorpyromorphite from Sukhovyaz and Tolbachik

Sukhovyaz (holotype)				Tolbachik (cotype)		hkl
I_{meas}	d_{meas}	I_{calc}*	d_{calc}	I_{meas}	d_{meas}	
5	8.370	1	8.486	8	8.450	100
10	4.910	9	4.889	5	4.939	110
25	**4.236**	27	4.243	**19**	**4.227**	200
15	4.041	43	4.063	**29**	**4.033**	111
3	3.638	6	3.636	11	3.660	002
30	**3.337**	30	3.342	**22**	**3.296**	102
28	**3.189**	19	3.207	**23**	**3.191**	210
100	**2.931**	100	2.935	**100**	**2.953**	112
20	**2.806**	54	2.829	**17**	**2.814**	300
5	2.443	1	2.450			220
8	2.243	6	2.173	8	2.209	113
5	2.122	7	2.121	7	2.109	400
15	2.035	42	2.032	**17**	**2.013**	222
18	1.943	29	1.934	7	1.936	123
48	**1.838**	42	1.832	**17**	**1.842**	402
5	1.667	6	1.671	2	1.676	204
14	1.590	11	1.593	7	1.595	331
		11	1.582	7	1.585	124
20	**1.534**	16	1.538	10	1.544	502
		12	1.530	8	1.527	304
12	1.485	18	1.490	6	1.482	332
8	1.330	6	1.332	5	1.340	521
13	1.295	16	1.296	8	1.291	414
10	1.270	12	1.270	5	1.265	252
4	1.222	8	1.222	5	1.219	440
12	1.177	6	1.178	3	1.167	116
5	1.146	6	1.147	2	1.141	352
8	1.057	1	1.058	1	1.052	800

*For the calculated patterns, only reflections with intensities ≥1 are given

7. Crystal structure

The structure of the holotype fluorpyromorphite was refined by the Rietveld method to $R_p = 0.1764$, R_{Bragg} (all) = 0.1352, R_F (all) = 0.0929 for 144 observed reflections. Rietveld refinement was carried out using Jana2020 software (Petříček et al. 2020) with the structural model taken from Mills et al. (2012) as a starting one, with F entirely replacing Cl in the case of fluorpyromorphite. Variables used were background modeled as the Legendre polynomials (manually defined 18 points suppressed by the fitted polynomial), zero-shift, *FWHM* function (for the pseudo-Voigt; *GW* and *LY*), preferred-orientation modeled as a March-Dollase function, unit-cell parameters, asymmetry according to Howard's term, and atom coordinates and displacement parameters of Pb atoms. Coordinates of all atoms other than Pb were kept fixed. The scaling is affected primarily by the atomic displacement parameters of the lead atoms. All refined and calculated values were corrected for correlations after Bérar and Lelann (1991). The summary of data collection conditions and refinement parameters are given in Tab. 4. The final Rietveld plot is displayed in Fig. 8. We have to emphasize that the quality of the Rietveld refinement is extremely limited; it should demonstrate here that the grain used is isostructural with pyromorphite, which has been proven with high confidence. However, the small grain size (300 μm) and pseudo-Gandolfi diffraction geometry led to relatively broad and weak diffraction profiles

Tab. 4 Summary of X-ray diffraction data collection conditions and structure refinement parameters for fluorpyromorphite (holotype)

Crystal data				
System	Hexagonal			
Space group	$P6_3/m$ (#176)			
Unit-cell parameters	a = 9.779(5) Å c = 7.241(9) Å			
Volume	599.6(7) Å^3			
Z	2			
Chemical composition	$Pb_5(PO_4)_3F$			
Density (calc.)	7.421			
μ (MoK_α)	70.44			
Source, radiation	Rigaku Supernova single-crystal X-ray diffractometer, Pilatus 200K detector; MoK_α			
2θ range for data collection [°]	2.57–37.63			
Refinement software	Jana2020			
Method	Rietveld			
Shape function; GW, LY	Pseudo-Voigt; 434(20), 62(8)			
Data/obs/restraints/parameters	3506/144/0/12			
R_p, R_{wp}	17.63, 16.46			
R_F, R_{Bragg}	9.29, 11.70			
GOF	0.07			
$\Delta\rho_{max}/\Delta\rho_{min}$	4.38, –8.06			
Refined atoms	*x*	*y*	*z*	U_{iso}
Pb1	0.333333	−0.333333	0.001(4)	0.017(3)
Pb2	0.2313(8)	−0.0143(15)	−0.25	0.0077(17)
P*	0.4104	−0.6215	−0.25	0.0156
O1*	−0.1437	0	0.25	0.0266
O2*	0.5248	0.1154	−0.25	0.0266
O3*	0.3616	−0.725	−0.0802	0.0266
F*	0	0	0.5	0.05

* – fixed

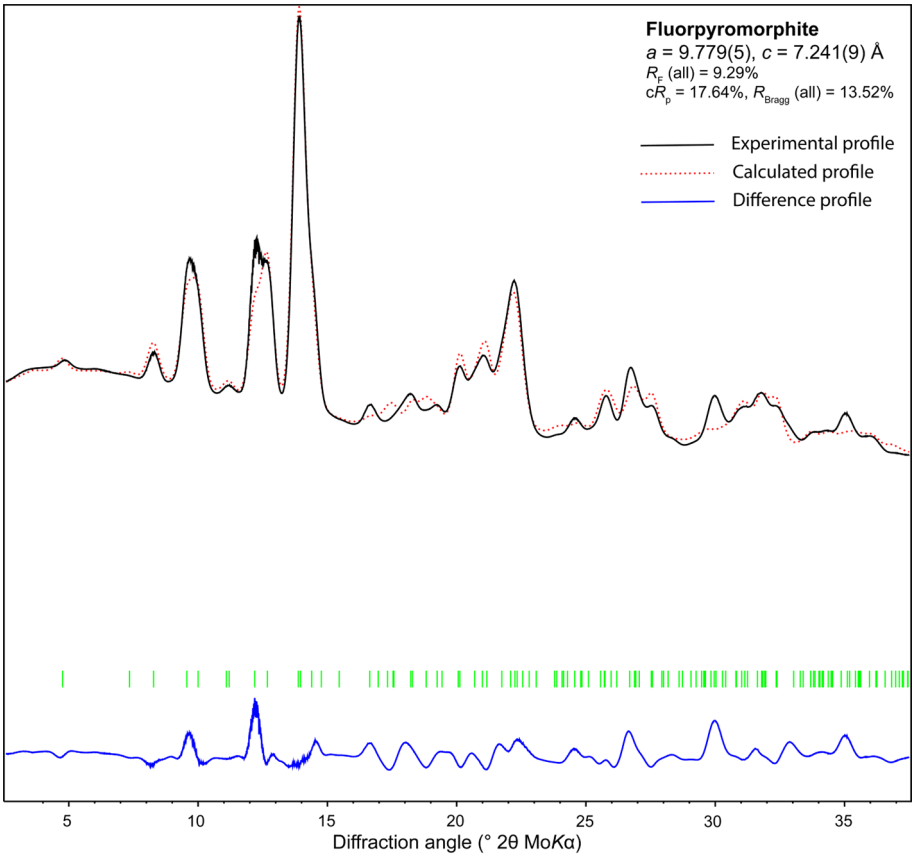

Fig. 8 Rietveld refinement plot for the holotype fluorpyromorphite.

Tab. 5 Comparative data of fluorpyromorphite, hydroxylpyromorphite and pyromorphite

Mineral	Fluorpyromorphite		Hydroxylpyromorphite	Pyromorphite*
	holotype	cotype		
End-member formula	$Pb_5(PO_4)_3F$		$Pb_5(PO_4)_3(OH)$	$Pb_5(PO_4)_3Cl$
Crystal system	Hexagonal			
Space group	$P6_3/m$			
a, Å	9.779(5)	9.732(1)	9.7872(14)	10.0017(19)
c, Å	7.241(9)	7.242(1)	7.3070(10)	7.3413(16)
V, Å^3	599.6(2)	594.0(2)	606.16(19)	636.0(2)
Z	2	2	2	2
Strongest lines of the powder X-ray diffraction pattern: *d*, Å – *I*, %	4.236–25 3.337–30 3.189–28 2.931–100 2.806–20 1.838–48 1.534–20	4.227–19 4.033–29 3.296–22 3.191–23 2.953–100 2.814–17 2.013–17	4.08–18 3.21–21 2.93–100 2.04–21 1.94–23 1.83–24 1.59–17	4.132–45 3.377–27 3.271–36 2.985–100 2.959–100 2.885–60 2.063–34
Density (calc.), g cm^{-3}	7.382	6.831	7.32	7.14
Source	This paper		Olds et al. (2021)	Dai and Hughes (1989), Hashimoto and Matsumoto (1998), Anthony et al. (2000), Mills et al. (2012)

* Unit-cell parameters are given after Mills et al. (2012) and powder XRD data and density after Anthony et al. (2000)

that prevented proper refinement of the positions of most atoms in the structure.

8. Discussion

Fluorpyromorphite is the fluorine-dominant analog of pyromorphite (Hausmann 1813; Dai and Hughes 1989; Hashimoto and Matsumoto 1998) and hydroxylpyromorphite (Olds et al. 2021). For a comparison of the three minerals, see Tab. 5.

While pyromorphite is a common secondary mineral found in the oxidation zone of many lead-bearing deposits, fluorpyromorphite and hydroxylpyromorphite are scarce. For example, the popular website Mindat (2022) cites more than 1800 localities from 62 countries for pyromorphite and only seven localities from four countries for hydroxylpyromorphite. The latter also occurs at Sukhovyaz Mt. as rare and tiny zones, up to 0.02×0.02 mm^2, in fluorpyromorphite grains. The most F, Cl-poor sample of Sukhovyaz hydroxylpyromorphite has the formula $Pb_{5.00}(PO_4)_3[(OH)_{0.57}Cl_{0.34}F_{0.09}]_{\Sigma 1.00}$, which is comparable to the holotype from Copps mine, Michigan, USA with the formula $Pb_{4.97}(PO_4)_3[(OH)_{0.69}F_{0.33}Cl_{0.06}]_{\Sigma 1.08}$ (Olds et al. 2021).

As for fluorpyromorphite, chemical compositions corresponding to this mineral were previously reported in the literature. Mikl and Kolitsch (2014) mentioned Ca-bearing "pyromorphite" with the F:Cl atomic ratio ~1.3 : 1 at Copper veins, Kleinelend glacier, Carinthia, Austria. Auer (2021) tentatively reported on "fluorpyromorphite" (3–4 at. % of F) from another Austrian locality – Ödenkar, Salzburger Land. However, none of the above phases were studied structurally and no attempts were made to describe them as a new mineral species. Olds et al. (2021) recorded a single spot electron microprobe analysis in the material from Copps Mine displaying an anomalously high F content (1.02 wt. %) which corresponds to the formula $Pb_{5.23}(PO_4)_3(F_{0.76}OH_{0.21}Cl_{0.08})_{\Sigma 1.04}$. This single analysis, however, was considered by the said authors to be of low quality due to the unreasonably high Pb : P and no further analyses have revealed any demonstrably F-dominant crystals.

The reason for the wide distribution of pyromorphite and the rarity of its fluorine- and hydroxyl-dominant analogs might be related to the presence of lead as the dominant cation at the **M** sites, which results in larger unit-cell dimensions and makes chlorine, whose ionic radius is markedly greater than those of fluorine and hydroxyl, the best candidate to occupy the **X** site (Pasero et al. 2010). The situation at Sukhovyaz Mt. is a good illustration: all three species are found there, but pyromorphite is abundant, while two others are found only as single rare grains or as small zones in individuals of the related minerals. Fluorapatite, commonly found at Sukhovyaz Mt. as inclusions up to 0.5 mm in quartz, obviously sourced the fluorine and contributed to the formation of fluorpyromorphite. Fluorpyromorphite forms partial pseudomorphs after fluorapatite: grains of the former contain relics of the latter. Thus, the formation of such an exotic mineral as a F-dominant member of the pyromorphite series is caused by the local enrichment of the mineral-forming medium by F^- mobilized from dissolved fluorapatite.

The appearance of fluorpyromorphite in products of the supergene alteration of fumarolic mineralization at the Tolbachik volcano also seems not unexpected: this mineral-forming system is, in general, F-rich, and thus local oversaturation in fluorine is very probable here. However, like at Sukhovyaz Mt., pyromorphite is much more widespread than fluorpyromorphite.

Noteworthy, another new F-dominant apatite-group mineral was recently discovered in paleo-fumarolic deposits of Mountain 1004, namely pliniusite $Ca_5(VO_4)_3F$.

Its holotype originates from the Southern paleo-fumarole field at the same scoria cone. Pliniusite forms here the continuous solid-solution system with svabite $Ca_5(AsO_4)_3F$ and fluorapatite (Pekov et al. 2022). However, these minerals do not contain Pb in detectable amount and have primary, sublimate origin in the oxidizing-type fumaroles, unlike the supergene lead apatite-group members – vanadinite, pyromorphite, fluorpyromorphite and fluorphosphohedyphane from the oxidation zone of the Western paleo-fumarole field. In addition, we see different compositions of **T** components in apatite-group minerals of different genesis here: the wide range of P–As–V substitutions in high-temperature calcium minerals *vs.* the limited P–Se–Cr substitutions in low-temperature lead halide–phosphates associated with P-depleted vanadinite.

Olds et al. (2021) suggested a possible solid-solution series between hydroxylpyromorphite and its fluorine-dominant analog. Actually, we found such a solid-solution system at Sukhovyaz Mt. In total, 108 chemical analyses were made and revealed both binary (F–OH, Cl–OH, F–Cl) and ternary (F–Cl–OH) substitutions, with 75 compositions matching pyromorphite, 29 fluorpyromorphite and only four hydroxylpyromorphite fields (Tab. 2, Fig. 9). The solid solution series between fluorpyromorphite and hydroxylpyromorphite extends from $Fpym_{96}Hpm_4$ to $Fpym_{61}Hpm_{39}$ with a gap in $Fpym_{79}Hpm_{21}$–$Fpym_{72}Hpm_{28}$ range. The series between pyromorphite and hydroxylpyromorphite extends from $Pym_{88}Hpm_{12}$ to $Pym_{51}Hpm_{49}$, with a small gap in the $Pym_{60}Hpm_{40}$–$Pym_{55}Hpm_{45}$ range. Finally, the solid solution in F–Cl binary substitution is rather limited: from $Pym_{81}Fpym_{19}$ to $Pym_{68}Fpym_{32}$. The ternary F–Cl–OH substitution occurs in almost half of the chemical analyses made (48 of 108). Finally, note that five analyses of pyromorphite from Sukhovyaz Mt. showed it to be chemically pure with respect to the anionic content, with 1 *apfu* Cl. The end-member compositions for tertiary substitutions are yet unknown for fluorpyromorphite and hydroxylpyromorphite.

Acknowledgments. We thank referees Travis Olds and Cristiano Ferraris for their valuable suggestions that helped to improve the manuscript. The editorial care of Martin Števko and Vojtěch Janoušek is greatly acknowledged as well. We are grateful to Mikhail Rassomakhin for his help with the Figure 2. This work was supported by the Russian Science Foundation, grant no. 19-17-00050 in part of the study of the Tolbachik material (IVP, NVC and NNK) and by the Operational Programme of the MEYS CR (Project No. SOLID21 CZ.02. 1.01/0.0/0.0/16_019/0000760). The technical support by the St. Petersburg State University X-Ray Diffraction Resource Center in the powder XRD study of Tolbachik fluorpyromorphite is acknowledged.

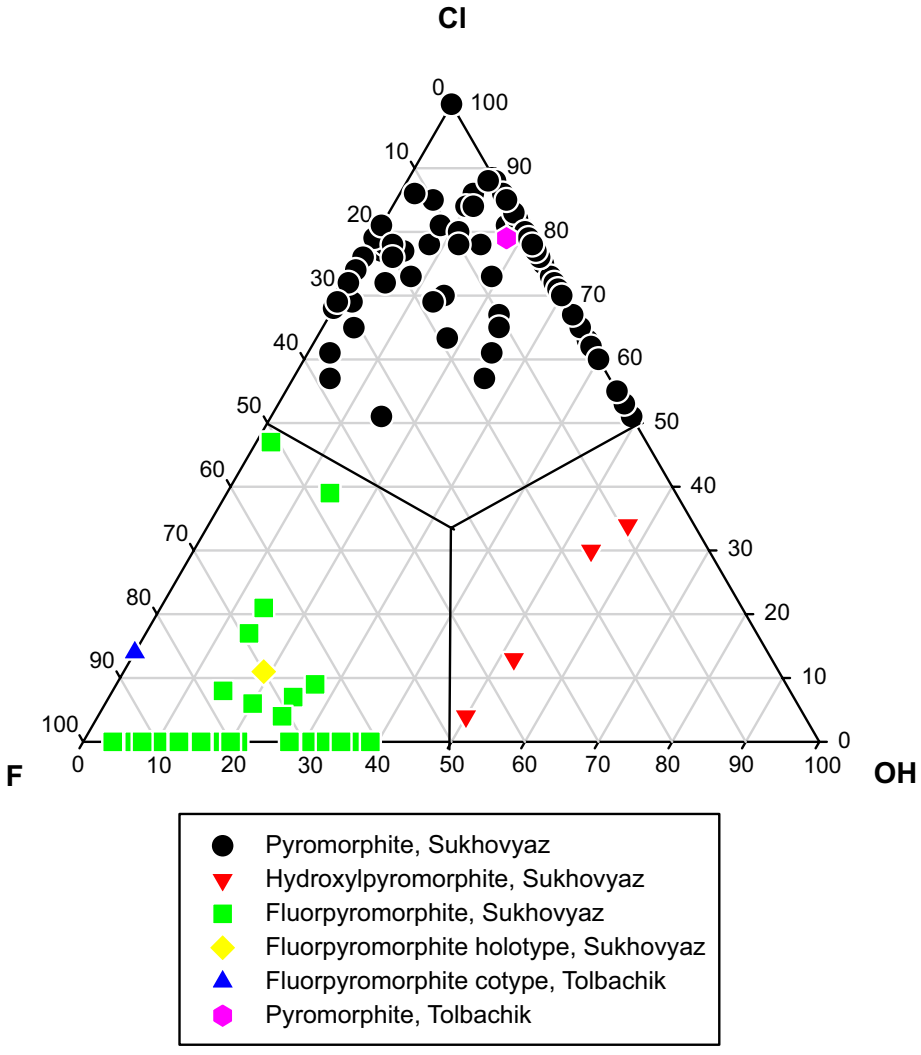

Fig. 9 Ternary plot of the F:Cl:OH ratios in fluorpyromorphite–pyromorphite–hydroxylpyromorphite solid-solution system minerals from Sukhovyaz Mt. and Tolbachik volcano.

References

Adams DM, Gardner IR (1974) Single-crystal vibrational spectra of apatite, vanadinite, and mimetite. J Chem Soc, Dalton Trans 14: 1505–1509

Anthony JW, Bideaux RA, Bladh KW, Nichols MC (2000) Handbook of Mineralogy. Volume IV. Arsenates, Phosphates, Vanadates. Mineral Data Publishing, Tucson, pp 1–680

Auer Ch (2021) Corkit, "Fluorpyromorphit"(?), Hidalgoit, "Hydroxylmimetesit", Tetradymit sowie ein weiterer Fund von Jarosit von den frühneuzeitlichen Bergbauhalden im Ödenkar, Radhausberg, Sportgastein, Salzburg. In: Walter F, Auer Ch, Bernhard F, Bojar H-P, Kandutsch G, Kiseljak R, Kolitsch U, Postl W, Schachinger T, Slama M, Trattner W, Weissensteiner G Neue Mineralfunde aus Österreich LXX. Carinthia II, 211–131_1, pp 222–224

Bajda T, Mozgawa W, Manecki M, Flis J (2011) Vibrational spectroscopic study of mimetite–pyromorphite solid solutions. Polyhedron 30: 2479–2485

Bartholomäi G, Klee WE (1978) The vibrational spectra of pyromorphite, vanadinite and mimetite. Spectrochim Acta A 34: 831–843

Bérar JF, Lelann P (1991) E.s.d.'s and estimated probable errors obtained in Rietveld refinements with local correlations. J Appl Crystallogr 24: 1–5

Botto IL, Barone VL, Castiglioni JL, Schalamuk IB (1997) Characterization of a natural substituted pyromorphite. J Mater Sci 32: 6549–6553

Britvin SN, Dolivo-Dobrovolsky DV, Krzhizhanovskaya MG (2017) Software for processing the X-ray powder diffraction data obtained from the curved image plate detector of Rigaku RAXIS Rapid II diffractometer. Zap Ross Mineral Obsh 146: 104–107 (in Russian)

Dai Y, Hughes JM (1989) Crystal structure refinements of vanadinite and pyromorphite. Canad Mineral 27: 189–192

Fedotov SA, Markhinin YK (eds) (1983) The Great Tolbachik Fissure Eruption. Cambridge University Press, NY, pp 1–341

Goldoff B, Webster JD, Harlow DE (2012) Characterization of fluor–chlorapatites by electron probe microanalysis with a focus on time-dependent intensity variation of halogens. Amer Miner 97: 1103–1115

Hashimoto H, Matsumoto T (1998) Structure refinements of two natural pyromorphites, $Pb_5(PO_4)_3Cl$, and crystal chemistry of chlorapatite group. Z Kristallogr 213: 585–590

Hausmann JFL (1813) Handbuch der Mineralogie. Vandenhoek & Ruprecht, Göttingen, pp 1–1158

Holland TJB, Redfern SAT (1997) Unit cell refinement from powder diffraction data: the use of regression diagnostics. Mineral Mag 61: 65–77

Levitt SR, Condrate RA, Sr (1970) Vibrational spectra of lead apatites. Amer Miner 55: 1562–1575

Merlet C (1994) An accurate computer correction program for quantitative electron probe microanalysis. Microchim Acta 114–115: 363–376

Mikl A, Kolitsch U (2014) Ein interessanter alpiner Kupfererzgang im Kleinelendtal und seine Mineralien. Mineralienwelt 25: 28–33

Mills SJ, Ferraris G, Kampf AR, Favreau G (2012) Twinning in pyromorphite: the first documented occurrence of twinning by merohedry in the apatite supergroup. Amer Miner 97: 415–418

Mindat. Accessed on December 2, 2022 at https://www.mindat.org

Olds TA, Kampf AR, Rakovan JF, Burns PC, Mills OP, Laughlin-Yurs C (2021) Hydroxylpyromorphite, a mineral important to lead remediation: Modern description and characterization. Amer Miner 106: 922–929

Pasero M, Kampf AR, Ferraris C, Pekov IV, Rakovan J, White TJ (2010) The nomenclature of the apatite supergroup minerals. Eur J Mineral 22: 163–179

Pekov IV, Agakhanov AA, Zubkova NV, Koshlyakova NN, Shchipalkina NV, Sandalov FD, Yapaskurt VO, Turchkova AG, Sidorov EG (2020) Oxidizing-type fumaroles of the Tolbachik volcano, a mineralogical and geochemical unique. Russ Geol Geophys 61: 675–688

Pekov IV, Koshlyakova NN, Zubkova NV, Krzątała A, Belakovskiy DI, Galuskina IO, Galuskin EV, Britvin SN, Sidorov EG, Vapnik Y, Pushcharovsky DY (2022) Pliniusite, $Ca_5(VO_4)_3F$, a new apatite-group mineral and the novel natural ternary solid-solution system pliniusite–svabite–fluorapatite. Amer Miner 107: 1626–1634

Pertel AI (1950) Pyromorphite from Sukhovyazskoe deposit in Urals. Proceedings of the G. V. Plekhanov Leningrad Mining Institute. Leningrad, Leningradskiy Gornyi Institut, pp 46–50 (in Russian)

Petříček V, Dušek M, Palatinus L (2020) Jana2020. The crystallographic computing system. Institute of Physics, Prague

Popov VA, Krainev YuD (2013) The shape of pyromorphite and crocoite crystals from the Sukhovyaz Mountain in the Southern Urals. In: Potapov SS (ed) Fourteenth All-Russian Scientific Readings in Memory of the Ilmen Mineralogist V.O. Polyakov. Miass, Institut Mineralogii Uralskogo Otdeleniya Rossiyskoy Akademii Nauk, pp 9–12 (in Russian)

Shchipalkina NV, Pekov IV, Koshlyakova NN, Britvin SN, Zubkova NV, Varlamov DA, Sidorov EG (2020) Unusual silicate mineralization in fumarolic sublimates of the Tolbachik volcano, Kamchatka, Russia – Part 1: Neso-, cyclo-, ino- and phyllosilicates. Eur J Mineral 32: 101–119

Stormer JC, Pierson ML, Tacker RC (1993) Variation of F and Cl X-ray intensity due to anisotropic diffusion

in apatite during electron microprobe analysis. Amer Miner 78: 641–648

Tait K, Ball NA, Hawthorne F (2015) Pieczkaite, ideally $Mn_5(PO_4)_3Cl$, a new apatite-supergroup mineral from Cross Lake, Manitoba, Canada: description and crystal structure. Amer Miner 100: 1047–1052

Vertushkov GN (1958) Plumbolimonite and pyromorphite from Verkhnyi Ufaley, Urals. Zap Vsesoyuz Mineral Obsh 87: 96–100 (in Russian)

Vlasov IA (2010) Mineralogy of Oxidation Zone of the Sukhovyazskoe Lead Deposit (Southern Urals). Faculty of Geology and Geophysics, Uralskiy Gosudarstvennyi Gornyi Universitet, Yekaterinburg, pp 1–55 (in Russian)

White T, Ferraris C, Kim J, Srinivasan M (2005) Apatite – an adaptive framework structure. In: Ferraris G, Merlino S (eds) Micro- and Mesoporous Mineral Phases. Mineralogical Society of America and Geochemical Society Reviews in Mineralogy and Geochemistry 57: 307–402